Proceedings of the 11th Brazilian Congress of Thermal Sciences and Engineering -- ENCIT 2006
Braz. Soc. of Mechanical Sciences and Engineering -- ABCM, Curitiba, Brazil,- Dec. 5-8, 2006

Paper CIT06-0670

NONLINEAR WAVE-CURRENT INTERACTIONS: THE GENERATION OF REFLECTED WAVES

Gabriel Nunes Coutinho & Roger Matsumoto Moreira
Computational Fluid Dynamics Laboratory (LabCFD)
School of Engineering, Fluminense Federal University
R. Passos da Pátria 156, bl.D, sl.563A, Niterói, R.J., Brazil. CEP: 24210-240.
E-mail: gncoutinho@gmail.com & roger@vm.uff.br

Abstract. *The interaction between wave groups on water surfaces and submerged currents is studied. This work was motivated by the constant change of the breaker line in the nearshore region caused by the irregular nature of the wave motion. For smooth monochromatic wavetrains, the nonlinear numerical results show that surface waves can be focused by adverse surface currents, leading to very rough water surfaces, with sometimes a partial reflection being observed; upstream of these regions the surface of the water is smooth as all short waves are eliminated. For bichromatic waves, the fully nonlinear results show that partial wave blocking occurs at the individual wave components in the wave groups and that waves become almost monochromatic upstream the blocking region. These results agree qualitatively with experiments conducted by Chawla (1999).*

Keywords*: Wave-current interactions, nonlinear effects, boundary integral method.*

1. Introduction

The interaction between wave groups and currents is of special importance when studying the effects of a moving blocking point. For instance, the excess momentum released by waves breaking on a beach acts as a forcing mechanism for fluid motion in the nearshore region. The breaker line is always moving due to the irregular nature of the wave motion and thus it is identified as one of the mechanisms for generating long waves in the coast. The temporally varying amplitude envelope of a narrow banded spectrum can create a moving blocking point.

The sharp steepening of waves prior to the blocking point makes the linear approach valid only for very small waves, which is not the case at river inlet entrances where waves are steep and tend to break at or before the blocking point. Several papers have been published based on data collected directly from the wave field. Wave height measurements in a tidal inlet were presented by Battjes (1982), while Gonzales *et al.* (1985) used SLAR imagery to estimate the wave height for slack and ebb currents at the Columbia river entrance. Other examples where measurements of water waves show correlation with the tides in areas of appreciable tidal currents are given by Vincent & Smith (1976) and Vincent (1979).

Due to the complexity of the wave field, experimental studies on this subject have also been performed. Sakai & Saeki (1984) conducted wave breaking tests for monochromatic waves in the presence of an opposing current but their experimental set up also included a sloping sea bed. The focus of their study was the combined effect of opposing currents and sloping sea bed on wave transformation and breaking, thus adding difficulties to isolate current limited wave breaking from depth limited wave breaking. Lai *et al.* (1989) conducted experimental studies with monochromatic and random waves on strong opposing currents. They limited their study to the kinematics of the wave-current interaction under blocking conditions and confirmed the dispersion relation and the implied reflection, but no measurements on amplitude variations were reported. Ris & Holthuijsen (1996) simulated current induced breaking and blocking with the help of a third generation wind wave spectral model and compared their results with the data of Lai *et al.* (1989). In all these experiments a very limited understanding of the wave energy dissipation due to current limited wave breaking was achieved.

Recent laboratory experiments using recirculating flumes have given a better understanding of the evolution of the wave field through the blocking region and the dynamics of the wave-current interaction. Chawla (1999) used a flume equipped with a perforated wavemaker to study the propagation of a series of monochromatic waves on an opposing blocking current. For very gentle waves, wave reflection from the blocking point was observed with the amplitude envelope confirming linear predictions. As the initial wave amplitude on a blocking current was increased, the wave envelope deviated from the Airy function theory and a transition region was identified between the case where waves are reflected from the blocking point with no breaking to the case where waves break at the blocking point with no reflection. Partial wave reflection was also observed in cases where the required blocking current is slightly greater than the maximum current. Chawla (1999) also carried on tests involving blocking of wave groups, obtained by modulating a carrier wave. His experimental results showed that blocking occurs separately for the individual wave components of the spectrum. However, his numerical simulations using a weakly nonlinear model showed that blocking occurs at the blocking point of the carrier wave instead. In addition, predictions of the blocking point were based on the linear

dispersion relation and thus could not account for nonlinear effects. The varied physical aspects in which wave-current interactions occur and the different mathematical approaches that are applicable to them can be found in the review papers of Peregrine (1976), Jonsson (1990) and Thomas & Klopman (1997).

Using a flume equipped with a wave generator and a perforated false bottom, Suastika *et al.* (2000) performed experiments on partial and complete wave blocking of periodic and random waves. For periodic wave tests, the incident wave steepness is seen to increase monotonically in the direction towards the blocking point. Reflection was also observed but with no systematic variation with the incident waves. The reflected wave steepnesses showed considerable scatter, which was interpreted as saturation due to wave breaking of the incident waves. Care should be taken in this case since the momentum lost from the waves in breaking is transferred to the current. Although this does not make a significant contribution to the mean current in deep water it certainly affects the current distribution in the surface layer that directly influences the waves. It is also important to notice that both Chawla (1999) and Suastika *et al.* (2000) generate turbulent currents with a constant mean velocity in relatively deep water. Reflection was also observed in the random wave tests. The reflected waves became more pronounced towards the blocking region, though the wave field was still dominated by the incident waves.

An amplitude evolution model based on the conservation of wave action, including dissipation and wave breaking, was also presented by Suastika *et al.* (2000). The spectral wave action balance was given by,

$$\frac{\partial}{\partial x}\left[\frac{E_n}{\Omega_n}\left(c_{g_n}+U\right)+\frac{D_n}{\Omega_n}\right]=0,$$

where Ω is the wave frequency in a reference frame moving with the current U, E is a spectral wave energy density in frequency space, D is a spectral wave energy dissipation and the subscript n refers to the n^{th} spectral component. A modified Battjes-Janssen model (Battjes & Janssen 1978) was used to model dissipation due to wave breaking while viscous dissipation along the sidewalls was introduced using the formulation of Hunt (1952). The model does not take into account the reflected waves and overestimated transmission through the blocking point. In the blocking region, model results showed significant discrepancies with observations. There is doubt in the literature about the value of using D_n. However, in the absence of better models, this is still employed.

To shed further light on the subject, we investigate through numerical simulations the behaviour of monochromatic and bichromatic gentle waves interacting with "rapidly" and "slowly" varying surface currents in deep water. In our simplified model the fully nonlinear, unsteady, boundary-integral method developed by Dold & Peregrine (1986) is modified in order to include the underlying current. The current is assumed to be two-dimensional and stationary, being induced by a distribution of singularities located beneath the free surface (Moreira & Peregrine 2001, Moreira 2001). The initial conditions for the boundary value problem are described in the following section.

2. Governing equation and boundary conditions

The free surface flow is assumed to be inviscid and incompressible. The singularities are distributed below the free surface in order to model the required underlying flow. The flow is supposed to be irrotational outside the singular cores and away from the free surface. The velocity field $\vec{u}(x,y,t)$ is given by the gradient of a full velocity potential $\Phi(x,y,t)$ which satisfies Laplace's equation in the fluid domain, excluding the singular points $\vec{x}_{S_i}$,

$$\nabla^2\Phi = 0, \qquad \text{in } D-\bigcup_{i=1}^{n}\vec{x}_{S_i}. \tag{1}$$

The fluid domain with its coordinates and parameters is illustrated in figure (1), with U representing a constant stream velocity.

The full velocity potential Φ is decomposed into a regular part ϕ_w (due to surface waves) and a singular part ϕ_s (due to the singularities),

$$\Phi=\phi_w+\phi_s, \tag{2}$$

which satisfies (1). The free surface´s kinematic and dynamic boundary conditions are given by,

$$\frac{D\vec{r}}{Dt}=\nabla\Phi, \tag{3}$$

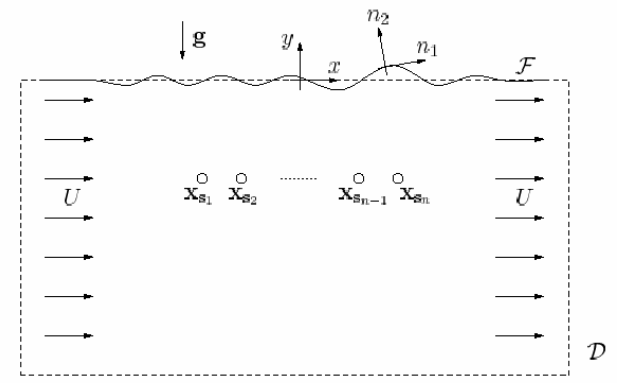

Figure 1. A sketch of the fluid domain *D* with its coordinates and parameters.

$$\frac{D\Phi}{Dt} = \frac{1}{2}|\nabla\Phi|^2 - \frac{p}{\rho} - gy \ . \tag{4}$$

$\vec{r}(x,y,t)$ is the position vector, y is the elevation of the free surface above the undisturbed water level, g is the acceleration due to gravity, ρ is the fluid density and p is the pressure on the exterior side of the surface. We assume deep water conditions i.e. $|\nabla\Phi| \to 0$ as $y \to -\infty$. To complete the boundary value problem an initial condition for the free surface is chosen,

$$\eta(x) = \eta_0(x), \qquad \Phi(x,\eta) = \Phi_0(x,\eta_0), \tag{5}$$

for $t = 0$. Attention is directed to two initial conditions: monochromatic wavetrains with initially uniform wavenumber K_0 and gentle steepness A_0K_0 (see figures 2a and 2b), and bichromatic waves produced by the addition of two wavetrains with same amplitude and slightly different wavenumbers and frequencies (figure 2c).

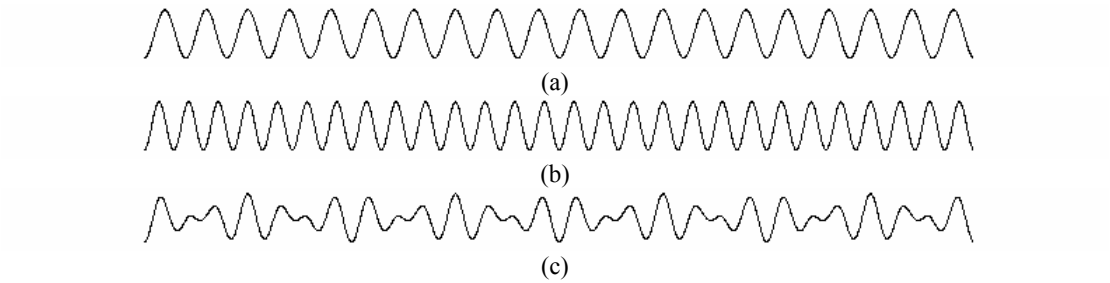

Figure 2. Monochromatic wavetrains with gentle steepness ($A_0K_0=0.04$) and initially uniform wavenumbers: (a) $K_0=10$; (b) $K_0=14$. When added together, they give the bichromatic wave (c).

3. Fully nonlinear boundary-integral solver

The boundary value problem is solved using an adapted version of the fully nonlinear potential flow program developed by Dold & Peregrine (1986), in which a boundary-integral method is applied to a free surface flow problem, reducing significantly the computational demand for the calculation of the fluid motion. The solution method is based on solving an integral equation that arises from Cauchy's integral theorem for functions of a complex variable. The original numerical scheme is modified for the inclusion of singularities. For details see Moreira & Peregrine (2001), Moreira (2001) and Moreira (2003).

The calculation of the free surface velocity $\nabla\phi_w$ becomes relatively simple when applying Cauchy's integral theorem. If we take $z = x + iy$ as the complex equivalent of the position vector $\vec{r} = (x,y)$ for a certain time t, ϕ_w is an analytic function of z. The wave complex potential gradient is defined as,

$$q_w = \frac{\partial \phi_w}{\partial x} - i\frac{\partial \phi_w}{\partial y}, \tag{6}$$

which is also an analytic function of z. On the boundary, z is treated as a function of the parameter ξ and time t. Similarly, taking $Z(\xi,t)$ as the complex equivalent of the surface profile vector $\vec{R}=(x(\xi,t),y(\xi,t))$, q_w can be defined in terms of the tangential and normal gradients of ϕ_w at the surface,

$$\overline{q}_w = \frac{\partial Z}{\partial n_1}\left(\frac{\partial \phi_w}{\partial n_1} + i\frac{\partial \phi_w}{\partial n_2}\right). \tag{7}$$

We assume that the surface contour C that surrounds the fluid domain is smooth; then applying Cauchy's integral theorem leads to,

$$\frac{\partial \phi_w}{\partial n_2} = \frac{1}{\pi}\oint_C \Im\left(\frac{\partial Z / \partial n_1}{Z' - Z}\right)\frac{\partial \phi_w'}{\partial n_2}\,dn_1' + \frac{1}{\pi}\oint_C \Re\left(\frac{\partial Z / \partial n_1}{Z' - Z}\right)\frac{\partial \phi_w'}{\partial n_1}\,dn_1', \tag{8}$$

in which $\partial\phi_w / \partial n_2$ can be determined since $\partial\phi_w / \partial n_1$ can be calculated directly. The arclength n_1' is a scalar variable which increases in an anticlockwise sense around the closed contour C. The primed variables Z', $\partial\phi_w' / \partial n_1$ and $\partial\phi_w' / \partial n_2$ are evaluated at points on the surface corresponding to n_1'.

The singularities distributed beneath the free surface can induce varied surface current profiles, each of them with a certain minimum and maximum velocity and with a gentle or sharp current gradient. Figures (3a) and (3b) show, respectively, surface current profiles obtained from a distribution of sinks/sources and an eddy couple. Here the peak velocities are related to c_0, the phase velocity of surface waves supposing no underlying current. Under the light of linear theory, a train of uniform linear water waves propagating with speed c_0 is expected to break when an adverse surface current reach velocities bigger than $0.25c_0$. For these situations, linear theory breaks down and no wave solution can be determined. A group of three different maximum and minimum velocities are presented: $0.25c_0$, $0.5c_0$ and c_0. In this case the singularity distributions were conveniently chosen aiming to define "slowly" and "rapidly" varying surface currents. For convenience the singularities are assumed to be at fixed positions in time such that steady surface currents are imposed on the waves. Hence waves do not affect the singularities in our nonlinear model. The effects of waves on vortices can be found in the works of Tyvand (1991), Tong (1991) and Barnes *et al.* (1996). The singularity distribution has to be weak enough for little or no effect on the waves such that their existence can be considered unimportant. The velocity potential ϕ_s then satisfies a linear equation beneath the surface. This condition is particularly relevant when "sharp" current gradients are considered.

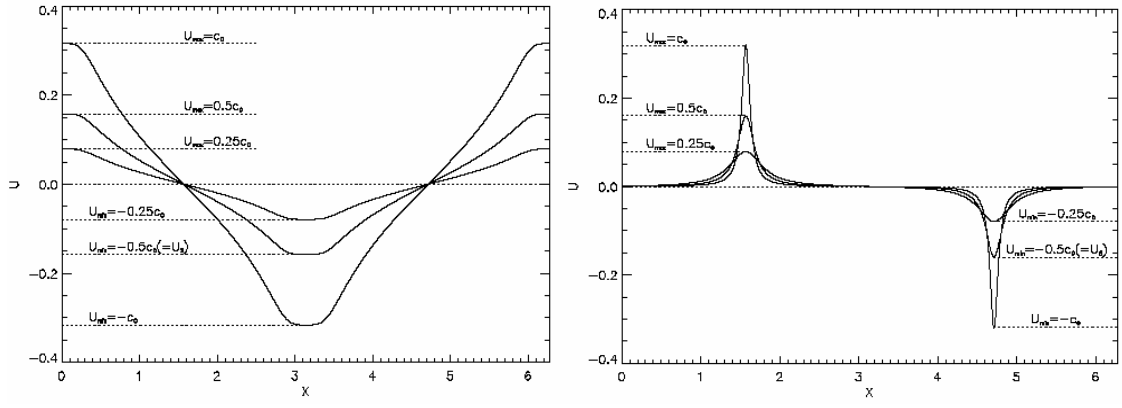

(a) (b)

Figure 3. Surface current profiles induced by: (a) 16 sinks and 16 sources (*Fr=0.015, 0.03, 0.06*); (b) an eddy couple (*Fr=0.08, 0.23, 0.64*).

The method of solution consists of the following stages. Initially the full potential Φ is known on the surface for each time step. The potential ϕ_s due to the singularities is also defined and subtracted from the surface value of Φ such that the remaining surface wave potential ϕ_w, which has no singularities in the fluid domain, can be used with Cauchy's integral theorem to calculate the velocity $\nabla\phi_w$ on the free surface. Then the potential ϕ_s is added back in and corresponding "total" velocities are evaluated. The inclusion of the singularities necessitates the computation of the partial derivatives with respect to *x* and *y* of the velocity potential ϕ_s up to the third derivative, since the time-step criterion uses a Taylor series expansion truncated at the sixth power. Since in our model the singularities are assumed at fixed positions, the partial time derivatives vanish. Once an accurate converged solution is obtained for the full velocity potential Φ on the free surface, the cycle can begin again. Such stages are repeated until either the final time is reached, or the algorithm breaks down. Full details can be found in Dold (1992).

In the calculation of surface waves by the numerical scheme, it is important that a sufficient number of surface points is used in order to guarantee the accuracy of the numerical method. Waves described by only a few surface points have their frequency and phase velocity underpredicted, with the percentage error decreasing rapidly the more points that describe each wavelength. However, an increase in the number of points used in the surface discretisation also leads to a significant increase in computing time and storage requirement. The surface discretisation points tend to drift due to the surface current induced by the singularities, soon developing poor resolution of the surface waves. To ensure a smooth variation of surface variables with point number, a redistribution of points along the surface at regular intervals in time is done by using a tenth-order interpolation algorithm. The computed cases presented here have an initial distribution of 120 points per wavelength for monochromatic waves and 350 points per wavelength of the carrier wave for bichromatic waves. To sum up no smoothing was introduced in the present computations in order to avoid any loss of information. The use of smoothing formulae based on the fitting of high order polynomials to the surface data was not required here since sawtooth numerical instabilities were well controlled by simply choosing an appropriate time step. Thus small waves with just two or three grid points and waves with sharp crests are not numerically dissipated by the scheme. All the computations presented in this work were done on a Intel Pentium 4 processor.

4. Fully nonlinear results

The fully nonlinear results presented in this section refer to monochromatic and bichromatic waves with initial gentle steepnesses interacting with surface currents induced by a distribution of singularities. "Slowly" and "rapidly" varying current gradients are obtained via a suitable distribution of sinks/sources and vortices beneath the free surface. A near-linear surface current is imposed with 16 sinks and 16 sources distributed symmetrically in the period domain at the same depth $d=0.25$. The effect of the singularity distribution on the waves then depends on the strength *k* of the sinks and sources. For convenience we define *k* as the volume flux per length unit of each of the sinks and sources. The desired maximum and minimum velocities are then obtained choosing suitable values for *k*. For "sharper" current gradients, a vortex couple is positioned underneath the free surface. In this case the peak velocities are defined by choosing suitable values for the depth of submergence *d*. The corresponding surface current profiles induced by these singularities are shown in figure (3). The stationary singularities are "turned on" at time $t=0$ and impose a volume flux perpendicular to the plane of motion. In the case of no surface current, surface waves propagate steadily without any distortion since the wave train is too gentle for the Benjamin-Feir instability to develop in the time available.

4.1. Monochromatic waves

Figure (4) shows the evolution of short surface waves ($A_0 K_0=0.04$) propagating over still water conditions and over near-linear and sharp surface current gradients ($U_{min}=-0.25\ c_0$). The nonlinear results are vertically exaggerated 40 times. It is clear from figures (4b) and (4c) the wave transformation that occurs due to the underlying current. A steep and a smooth region can be identified, respectively, downstream and upstream of the U_{min} region after a certain period of time. A strong increase in wave steepness is observed close to the U_{min} region, leading to wave breaking, while wave amplitudes decrease beyond this region. Some of the waves are steep enough to be noticeably affected by nonlinearity. Partial wave blocking is predicted by linear ray theory and thus confirmed by the nonlinear computations. The incident waves are clearly deformed near the maximum and minimum velocity regions U_{max} and U_{min}, while their group velocity remains unchanged near the regions where $U=0$. The positive current accelerates the surface waves nearby the U_{max} region, increasing locally their kinetic energy and group velocity, while in the U_{min} neighbourhood waves start to be partially blocked. When stronger currents are imposed, nonlinear effects take over with wave breaking occurring sooner nearby the U_{min} region.

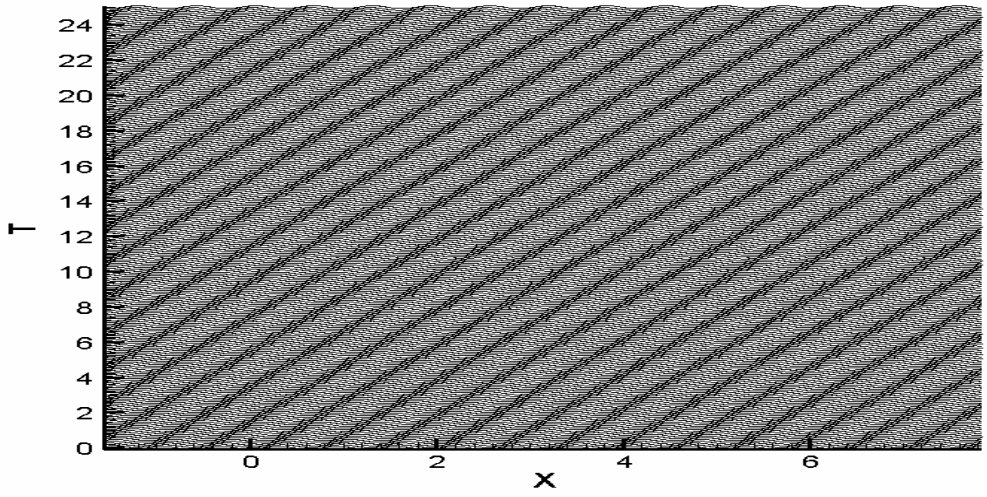

(a)

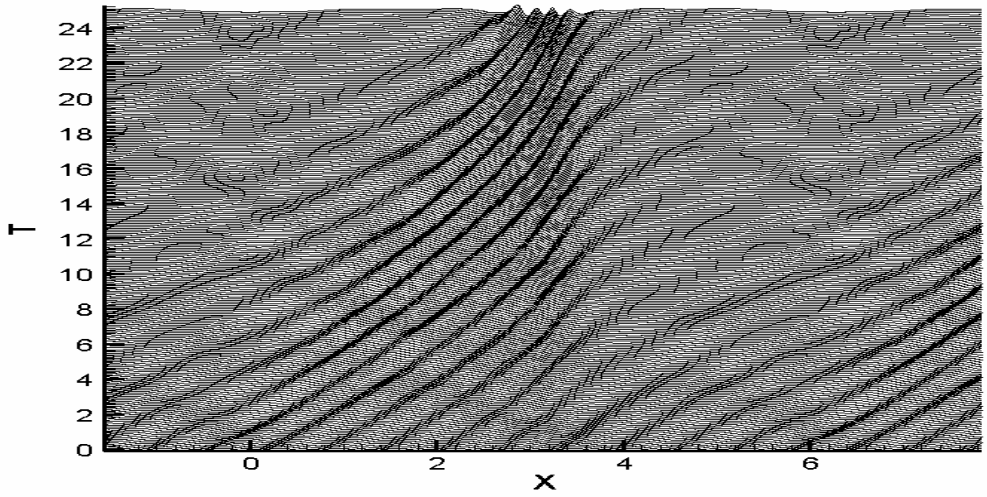

(b)

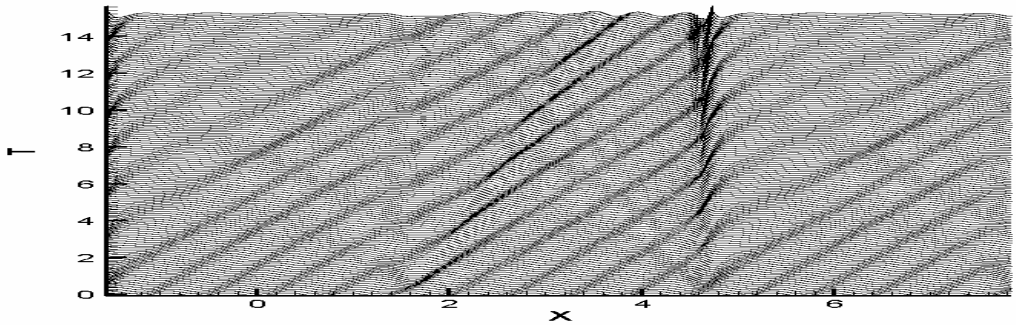

(c)

Figure 4. Free surface evolution of monochromatic waves over: (a) no underlying current; (b) a near-linear current ($t_{breaking}=25.4$); (c) a vortex current ($t_{breaking}=14.8$). $U_{min}=-0.250\ c_0$, $K_0=10$, $A_0\ K_0=0.04$. Vertical exaggeration 40:1.

4.2. Bichromatic waves

Chawla (1999) conducted a series of experiments on narrow banded spectral waves to study if it was possible to similarly generate long waves downstream of a moving blocking point. As already explained in section 1, his experimental results showed that this was not the case, with blocking occurring separately for the individual wave components of the spectrum, while his numerical simulations showed that blocking occurs at the blocking point of the carrier wave instead. Predictions of the blocking point were based on the linear dispersion relation and thus could not account for nonlinear effects. A Boussinesq model for wave blocking also shows a similar effect but is limited due to inaccuracies in its dispersive properties in deep water (Chen *et al.* 1998).

To shed further light in the matter, the numerical scheme proposed in section 3 was used to simulate the interactions between wave groups and currents. The wave groups were constructed by superposing two monochromatic waves having the same amplitude but slightly different frequencies, with the difference between the frequencies determining the number of waves in a group. This spectral approach was also employed by Chawla (1999). Based on his cleanest wave groups i.e. bichromatic waves with no energy transferred to the side bands, we set up our initial condition by superposing two uniform wave train components with $A_0\, K_0=0.06$, 0.084 and $K_0=10$, 14, respectively.

The evolution of these wave groups over "slowly" and "rapidly" varying currents is shown respectively in figures (5b) and (5c). For comparison purposes wave groups propagating over still water are presented in figure (5a). These nonlinear results show that partial wave blocking can occur at the individual wave components in the wave groups and that waves become almost monochromatic beyond the U_{min} region, which is clear from figure (5b). Unfortunately the numerical computations stop due to wave breaking. Wave reflection was not observed. Comparisons with solutions of the nonlinear Schrödinger equation are under development.

5. Summary

We have attempted to simulate the interaction between water waves and currents with special attention to the effects of nonlinearity on the free surface. This was motivated by several theoretical and recent experimental works on the matter. A fully nonlinear model was developed in order to understand the interaction of stationary submerged currents induced by singularities with gentle wavetrains and wave groups. The nonlinear numerical results show that adverse currents induce wave steepening and breaking. Furthermore the wave transformation induced by the underlying currents can be identified by a steep and a smooth region formed, respectively, downstream and upstream the blocking point after a certain period of time. A strong increase in wave steepness is observed within the blocking region, leading to wave breaking, while wave amplitudes decrease significantly beyond this region. In the case of interactions between wave groups and currents, the fully nonlinear results show that wave blocking can occur for the individual wave components in the wave groups and that waves evolve from being groupy to being almost monochromatic, confirming qualitatively the experimental observations of Chawla (1999).

6. Acknowledgement

Gabriel Nunes Coutinho acknowledges the financial support through FAPERJ. This research is supported by CNPq under contract no. 62.0018/2003-8-PADCT III / FAPERJ.

7. References

Barnes, T.C.D., Brocchini, M., Peregrine, D.H. & Stansby, P.K., 1996, "Modelling post-wave breaking turbulence and vorticity." *Proc. 25th Internat. Conf. on Coastal Engng.*, Orlando, ASCE, v.1, pp.186-199.

Battjes, J.A., 1982, "A case study of wave height variations due to currents in a tidal entrance." *Coastal Engineering*, v.6, pp.47-57.

Battjes, J.A. & Janssen, J.P.F.M., 1978, "Energy loss and set-up due to breaking of random waves." *Proc. 16th Internat. Conf. on Coastal Engng.*, Hamburg, ASCE, pp.569-587.

Chawla, A., 1999, "An Experimental Study on the Dynamics of Wave Blocking and Breaking on Opposing Currents." PhD thesis, University of Delaware, U.S.A.

Chen, Q., Madsen, P.A., Schäffer, H.A. & Basco, D.R., 1998, "Wave-current interaction based on an enhanced Boussinesq approach." *Coastal Engineering*, v.33, pp.11-39.

Dold, J.W., 1992, "An Efficient Surface-Integral Algorithm Applied to Unsteady Gravity Waves." *J. Comp. Phys.*, v.103, pp.90-115.

Dold, J.W. & Peregrine, D.H., 1986, "An Efficient Boundary-Integral Method for Steep Unsteady Water Waves." In *Numer. Meth. for Fluid Dynamics II*, Eds. K.W. Morton & M.J. Baines, pp.671-679.

Gonzales, F.I., Cokelet, E.D., Gower, J.F.R. & Mulhern, M.R., 1985, "SLAR and in-situ observations of wave-current interaction on the Columbia River Bar." In *The Ocean Surface*, Eds. Y. Toba & H. Mitsuyasu, pp.303-310.

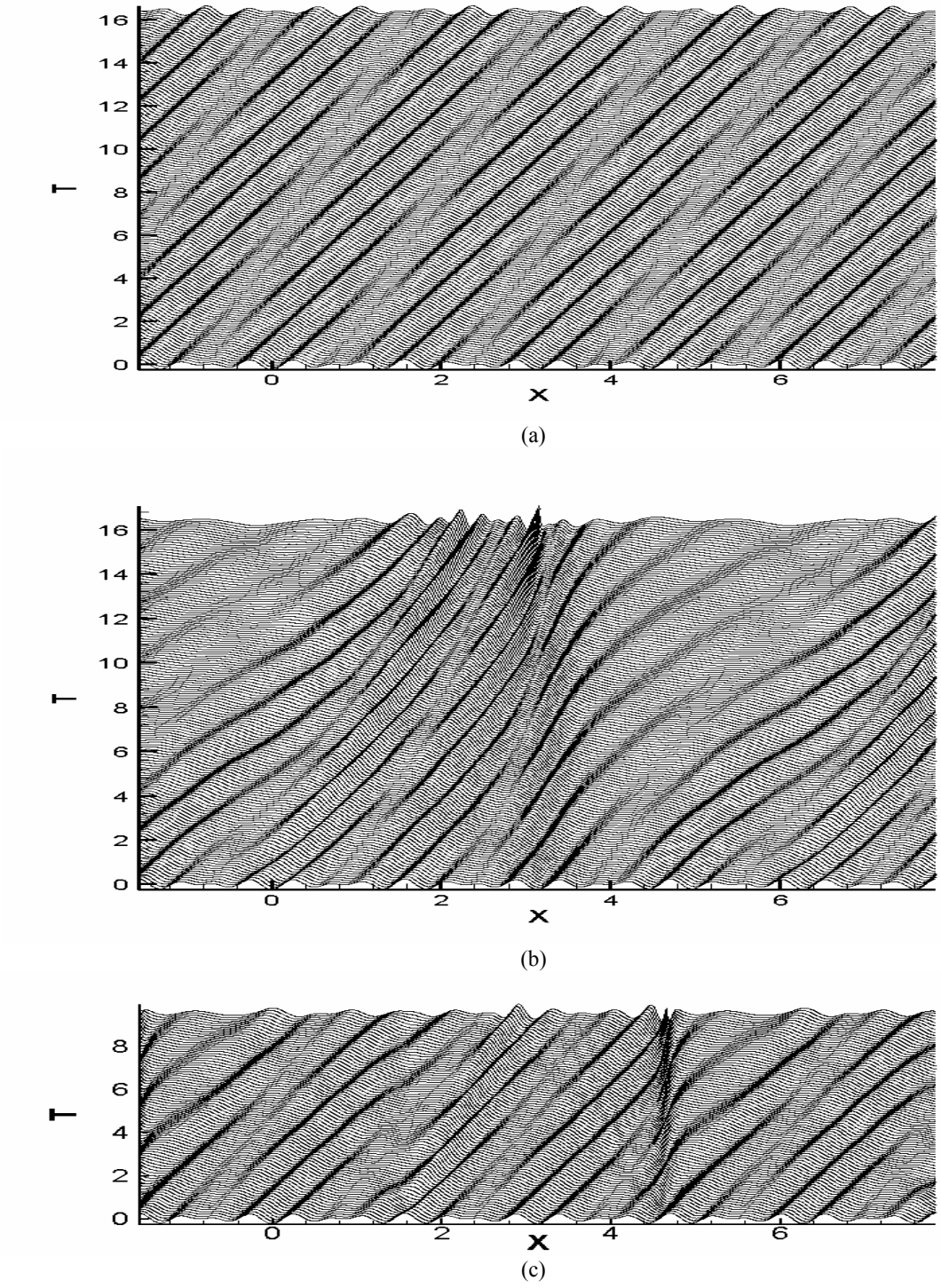

(a)

(b)

(c)

Figure 5. Free surface evolution of bichromatic waves over: (a) no underlying current; (b) a near-linear current ($t_{breaking}$=*16.4*); (c) a vortex current ($t_{breaking}$=*9.5*). U_{min}=*-0.250* c_0; K_0=*10, 14;* A_0 K_0=*0.06, 0.084*. Vertical exaggeration 40:1.

Hunt, J.N., 1952, "Viscous damping of waves over an inclined bed in a channel of finite width." *La Houille Blanche*, pp. 837-842.

Jonsson, I.G., 1990, "Wave-current interactions." In *The Sea*, Ocean Engng. Science 9A, Eds. B. Le Mehaute & D.M. Hanes, pp.65-120.

Lai, R.J., Long, S.R. & Huang, N.E., 1989, "Laboratory studies of wave-current interaction: Kinematics of the strong interaction." *J. Geophys. Res.*, v.94, pp.16201-16214.

Moreira, R.M., 2001, "Nonlinear interactions between water waves, free surface flows and singularities." PhD thesis, University of Bristol, U.K.

Moreira, R.M. & Peregrine, D.H., 2001, "Interactions between water waves and singularities." In *IUTAM Symp. on Free Surface Flows*, Eds. A.C. King & Y.D. Shikhmurzaev, pp.205-212.

Moreira, R.M., 2003, "Nonlinear interactions between water waves and currents." *Proc. 6th Internat. Conf. on Coastal & Port Engng. in Developing Countries*, Colombo, pp.1-10.

Peregrine, D.H., 1976, "Interaction of water waves and currents." *Adv. Appl. Mech.* 16, pp.9-117.

Ris, R.C. & Holthuijsen, L.H., 1996, "Spectral modelling of current induced wave-blocking." Proc. *25th Internat. Conf. on Coastal Engng.*, Orlando, ASCE, pp.1246-1254.

Sakai, S. & Saeki, H., 1984, "Effects of opposing current on wave transformation." *Proc. 19th Internat. Conf. on Coastal Engng.*, Houston, ASCE, pp.1132-1148.

Suastika, I.K., de Jong, M.P.C. & Battjes, J.A., 2000, "Experimental study of wave blocking." *Proc. 27th Internat. Conf. on Coastal Engng.*, Sydney, ASCE, pp.223-240.

Thomas, G.P. & Klopman, G., 1997, "Wave-current interactions in the nearshore region." In *Gravity Waves in Water of Finite Depth*, Ed. J.N. Hunt, pp.215-319.

Tong, R.P., 1991, "Unsteady Flow with a Free Surface: A Study of Numerical Approximations in the Boundary Integral Method." PhD thesis, University of Bristol, U.K.

Tyvand, P.A., 1991, "Motion of a vortex near a free surface." *Journal of Fluid Mechanics*, v.225, pp.673-686.

Vincent, C.E., 1979, "The interaction of wind-generated sea waves with tidal currents." *Journal of Physical Oceanography*, v.9, pp.748-755.

Vincent, C.E. & Smith, D.J., 1976, "Measurements of waves in Southampton water and their variation with the velocity of the tidal current." *Estuarine Coastal Mar. Sci.*, v.4, pp.641-652.

8. Responsibility notice

The authors are the only responsible for the printed material included in this paper.